In situ hydrogelation of photocurable gelatin and drug release

H. Okino,[1,3] Y. Nakayama,[2] M. Tanaka,[1] T. Matsuda[3]
[1]*Department of Surgery and Oncology, Graduate School of Medicine, Kyushu University, 3-1-1 Maidashi, Higashiku, Fukuoka 812-8582, Japan*
[2]*Department of Bioengineering, National Cardiovascular Center Research Institute, 5-7-1 Fujishirodai, Suita, Osaka 565-8565, Japan*
[3]*Department of Biomedical Engineering, Graduate School of Medicine, Kyushu University, 3-1-1 Maidashi, Higashiku, Fukuoka 812-8582, Japan*

Received 16 April 2001; accepted 5 June 2001
Published online 2 November 2001; DOI 10.1002/jbm.1237

Abstract: We devised an *in situ* tissue-adhesive, drug-release technology based on a photoreactive gelatin, which allows *in situ* drug-incorporated gel formation on living tissues and sustained drug release directly on diseased tissues. Styrene-derivatized gelatins, synthesized by condensation reaction of gelatin with 4-vinylbenzoic acid, were photopolymerized in the presence of a water-soluble camphorquinone derivative as a photoinitiator upon visible-light irradiation to form swollen gels. Using albumin as a drug model, gelation characteristics and drug-release characteristics easily were manipulated by material variables, formulation variables, and operation variables. Tissue adhesivity of the gel was superior to that of fibrin glue. The biologic response, which was evaluated by intraperitoneal implantation in rats, showed that the gel was biodegraded and biosorbed, without cytotoxicity, within a few months after implantation. An *in situ* processable tissue-adhesive local drug release system effectively may be used to help inhibit tumor recurrence. © 2001 John Wiley & Sons, Inc. J Biomed Mater Res 59: 233–245, 2002

Key words: photoreactive gelatin; hydrogel; visible-light irradiation; local drug delivery

INTRODUCTION

Advanced malignant-tumor recurrence caused by remnant malignant cells occurs at a high rate even after radical surgery. Although systemic adjuvant chemotherapy can be and often is performed after surgery, it does not necessarily contribute to a reduction of the recurrence rate. If a system capable of directly delivering a drug to a target tissue for a prolonged period were to be developed and applied to diseased tissues immediately after surgery, it might lead to maximum therapeutic benefits while minimizing the systemic side effects.

This study was presented at the XXVIIth Congress of the European Society of Artificial Organs, Lausanne, Switzerland, August 31–September 2, 2000.

Correspondence to: T. Matsuda; e-mail: matsuda@med.kyushu-u.ac.jp

Contract grant sponsor: Organization for Pharmaceutical Safety and Research (OPSR); contract grant number: Promotion of Fundamental Studies in Health Science, Grant No. 97-15

Such a tissue-directed drug delivery system for this purpose would have several requirements. First, a drug-immobilizing, insoluble matrix would have to be developed, one that would adhere well on living tissues. Second, the immobilized drug would have to be sustainedly released over time. Third, after a desired time period, the matrix would have to biodegrade and biosorb.

To this end, *in situ* photopolymerization techniques have advantages over conventional chemical crosslinking methods for the following reasons: (1) the desired amount of drug in a photocured matrix can be easily loaded; (2) the crosslinking density, which may affect the drug-release rate, can be controlled; and (3) *in situ* photopolymerization enables the formation of a drug-loaded tissue-adhesive matrix on diseased tissue. Based on these requirements, we devised a visible-light-driven photocurable drug-release technology, as described later.

Recently, the photopolymerization technique has been employed in biomedical applications because it enables the rapid conversion of a photoreactive monomer or macromer solution into gels or solids under

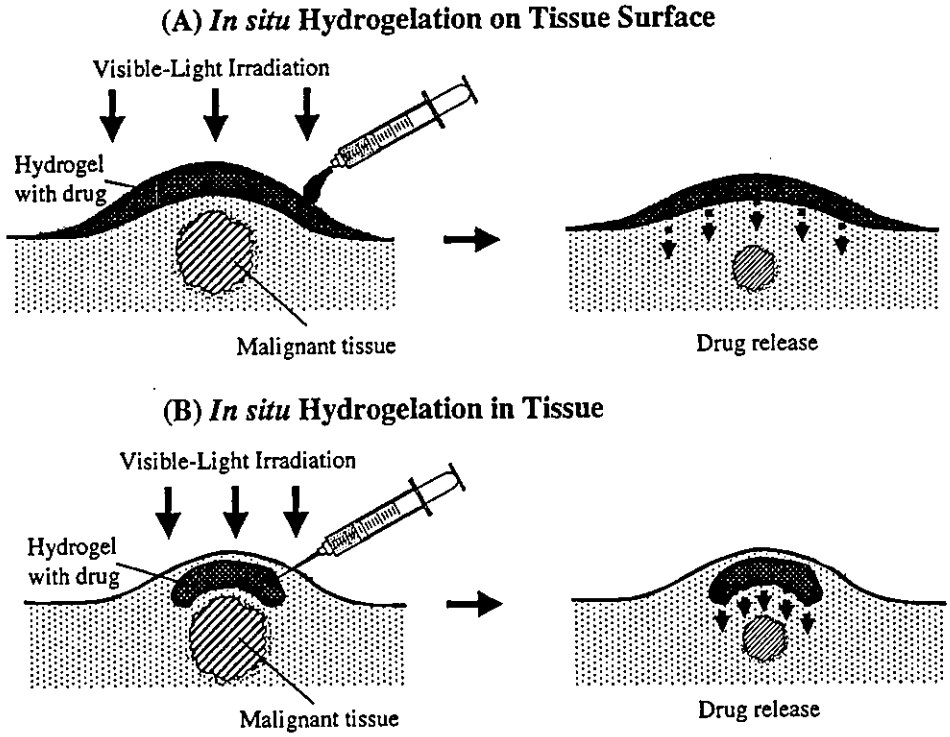

Figure 1. Schematic of *in situ* photocurable drug-release technology to prevent recurrence of malignant tissues: (A) hydrogelation on tissue surface; (B) hydrogelation in tissue.

physiologic conditions *in situ* with minimal invasion. Various hydrogels for use in local drug delivery systems were synthesized by a photopolymerization technique using mono-, di- or multifunctional vinylated monomer or macromers, such as 2-hydroxyethyl methacrylate,[1-3] poly(ethylene glycol) di(meth)acrylate,[4-6] poly(ethylene glycol)-co-poly(lactic acid) block copolymer terminated with (meth)acrylate at both ends,[7] methacrylated dextran,[8] oligo(ethylene glycol) multiacrylates,[9] and styrenated gelatin.[10,11]

As one application of multifunctional styrene-derivatized gelatin, which originally had been developed for photocurable tissues by us,[11] the potential of an *in situ* drug delivery system is assessed here for the treatment of cancer by local chemotherapy. A newly designed and conceptual therapeutic procedure for fully utilizing the photocuring characteristics of gelatin by visible-light irradiation, which leads to the formation of a drug-release reservoir on as well as in diseased tissues, is shown schematically in Figure 1. Figure 2(A) shows the schema of photoreactive gelatin, in which styrene groups multiply were derivatized via the amino groups of lysine residues of gelatin.

Water-soluble carboxylated camphorquinone, which produces radicals upon visible-light irradiation, served as the initiator for radical polymerization. Inter- and intramolecular polymerizations of styrene groups in gelatin molecules lead to the formation of a crosslinked gelatin network, producing a water-swollen gel [Fig. 2(B)]. An immobilized drug, when

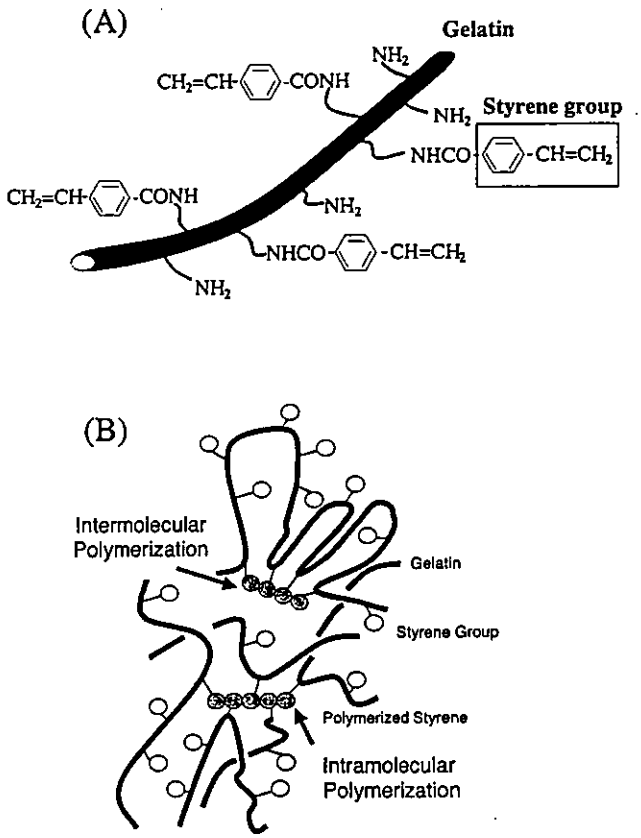

Figure 2. Photocurable gelatin and its photogelation: (A) chemical structure of styrene-derivatized gelatin; (B) photogelation mechanism by formation of crosslinked gelatin networks by the intermolecular and intramolecular polymerizations of styrene groups in gelatin molecules.

premixed in a photocurable system prior to photoirradiation, may be released from the gel, and swelling and enzymatic and/or immunocompetent cell-induced biodegradation may accelerate drug release. It is conjectured that both the drug release rate and the release period are controlled by the physical structure of the gel.

The objective of this study was to develop an *in situ* tissue-adhesive drug-release system using a styrene-derivatized gelatin, whereby a gel is formed on the living tissue after a few minutes of visible-light irradiation, immobilizing the drug and subsequently allowing the sustained release of the drug to the tissue in contact with the photocured gel. As the first article in a series of studies, this study focuses on the fundamental aspects of gelation characteristics and the *in vitro* performance of the gel as tissue-adhesive, drug-releasable matrix, and it is divided into three sections. First, gelation characteristics of the photoreactive gelatin are described; second, release characteristics of albumin as the model proteinaceous drug from the gel are determined; and third, tissue-adhesive strength for application is measured. The potential application of the gel to postoperative cancer chemotherapy is discussed.

MATERIALS AND METHODS

Materials

Gelatin (from bovine bone, MW 9.5×10^4) was obtained from Wako Pure Chem. Ind., Ltd., (Osaka, Japan). Water-soluble camphorquinone (CQ) was prepared according to the method described previously.[10] Dye-conjugated proteins, rhodamine-lactalbumin and rhodamine-albumin, were obtained from Sigma Chemical Co. (St. Louis, MO). Rhodamine goat anti-mouse IgG was purchased from Molecular Probes (Eugene, OR). Acid-solubilized bovine dermal type-I collagen solution was purchased from Koken Corp. (CELLGEN, Tokyo, Japan).

Synthesis of styrene-derivatized gelatin

Styrene-derivatized gelatins with different degrees of derivatization were synthesized according to the procedure reported previously.[11] The gelatins with different degrees of derivatization were prepared with various concentrations of 4-vinylbenzoic acid (Tokyo Kasei Kogyo, Co., Ltd., Tokyo, Japan) while all the other parameters were fixed. The typical procedure was as follows: 4-vinylbenzoic acid (5.7 g, 38.5 mmol) was dissolved in 400 mL of an aqueous sodium hydroxide solution (0.1*N*) and then neutralized to pH 7.5 with 1.0*N* of hydrochloric acid. To the aqueous solution, 500 mL of a phosphate-buffered saline solution (PBS; pH 7.4; Nissui Pharmaceutical Co., Ltd., Tokyo, Japan) of gelatin (10.0 g) was added, and the mixture was stirred for 30 min on ice. After the addition of 1-ethyl-3-(3-dimethylaminopropyl)carbodiimide hydrochloride (WSC; 14.8 g, 77.2 mmol; Dojindo Laboratories, Kumamoto, Japan), the solution was stirred for 24 h at room temperature. The reaction mixture was dialyzed using a seamless cellulose tube (Dialysis Membrane, Size 36, Wako Chemicals USA, Inc., Richmond, VA) in water for 3 days and then lyophilized using a freeze-drier (FZ-1, Labconco, Kansas, MO) under reduced pressure. A white cotton-like substance was obtained. The number of styrene groups incorporated into a gelatin molecule was calculated based on its absorbance as determined using a UV/Vis spectrophotometer (DU530, Beckman, Fullerton, CA), and the degree of derivatization (DD) was calculated using these values, based on the maximum number of amino groups in the lysine residues (36.8 per mol), which was determined using the trinitrobenzene sulfonate (TNBS) method.

Preparation of aqueous gelatin solution

A typical example of preparation of an aqueous gelatin solution is as follows: PBS solution containing styrene-derivatized gelatin and carboxylated camphorquinone (CQ) was stirred thoroughly with a high-speed rotating shaker (MX-201, Thinky Co., Ltd., Tokyo, Japan) and subsequently degassed at 40°C for 30 min.

Visible-light irradiation

Visible-light irradiation was carried out using an 80-W halogen lamp (Tokuso power lite, Tokuyama Co. Ltd., Tokuyama, Japan). The wavelength of illumination ranged from 400 to 520 nm. Light intensity as measured with a photometer (ANA-F11, Tokyo Kohden Co., Ltd., Tokyo, Japan) was 1.3×10^6 lx.

Gel yield and degree of swelling

An aqueous gelatin solution (100 μL; weight of the solid content: W_{solid}) containing 0.05 wt % CQ was poured onto a circular glass coverslip (diameter, 18 mm) and then irradiated for a predetermined time. After removing the nonreacted substances by soaking in PBS at 60°C for 20 min, the disk-shaped gels ob-

tained were equilibrated in PBS for 24 h at room temperature and then weighed (W_{water}) after excess water carefully was removed. The vacuum-dried gels were weighed (W_{gel}). The gel yield (%) was calculated using the equation

$$W_{gel} / W_{solid} \times 100$$

and the degree of swelling (DS) was calculated as

$$W_{water} - W_{gel}/W_{gel}.$$

Determination of drug release

One hundred and fifty mg of aqueous gelatin solution containing 0.05 wt % CQ and dye-conjugated protein, as mentioned below, was poured onto the bottom of a cuvette (Kartel, Milano, Italy), and a photocurable gel was prepared by exposure to 1.3×10^5 lx of visible-light for 3 min. After adding 3 mL of PBS (pH 7.4) supplemented with penicillin, streptomycin, and fluconazole into the cell, liquid samples were withdrawn from the cuvettes at regular intervals at room temperature. The concentrations of dye (rhodamine)-conjugate proteins, such as lactalbumin (MW: 1.4×10^4), albumin (MW: 6.6×10^4), and IgG (MW: 1.6×10^5), were fixed at 2 wt % of the total mixture. The amount of rhodamine-conjugated proteins released from the gel was determined spectrophotometrically. The maximum absorbance of the drug solutions was detected at 558 nm for lactalbumin, 595 nm for albumin, and 572 nm for IgG, respectively.

Determination of apparent diffusion coefficient

The apparent relative diffusion coefficients were determined according to Fick's second law of diffusion as follows.[12]

$$\frac{M_t}{M_\infty} = \frac{4}{\sigma}\left(\frac{Dt}{\Pi}\right)^{1/2}$$

Here, M_t is the amount released from the gel at any time, M_∞ is the total amount released at infinite time, D is diffusion coefficient, t is the time and δ is the half thickness of the gel.

Viscosity

The viscosity of aqueous solutions of the styrene-derivatized gelatin at 25° and 37°C was measured with a viscometer (TV-20, TOKIMEC, Tokyo, Japan).

Tissue adhesion

The shear adhesive strength of the gel coated on a moisturized collagen film (collagen casing, Nippi Inc., Tokyo, Japan) as the model tissue was measured using a rheometer (RheonerII, Yamaden, Tokyo, Japan). Onto the collagen film, which was equilibrated in PBS at room temperature and subsequently wiped of excess water, 100 μL of aqueous gelatin solution was poured, followed by photoirradiation for 3 min. The collagen film was fixed on the sample holder table, and then the produced gel was fixed with a plunger using cyanoacrylate as the adhesive. A plunger was moved apart from the collagen film in distilled water at a rate of 1 mm/s. The maximum stress was defined as an adhesive strength.

SEM observation

The specimens were fixed in a fixative (2% glutaraldehyde in 0.1-*M* cacodylate buffer, pH 7.4) for 2 h at room temperature and rinsed with buffer five times. They were postfixed with 1% osmium tetroxide in buffer for 2 h, washed with buffer five times, stained with 1% tannic acid for 30 min, and washed with distilled water five times. Subsequently, they were dehydrated with a graded series of ethanol, critical-point dried, sputter-coated with platinum, and evaluated by scanning electron microscopy (SEM) (JEOL, JSM-6301F, Tokyo, Japan).

Tissue permeability

A disk-type hybrid tissue (diameter, 10 mm; thickness, 1 mm), which was the fibroblast-immobilized collagen gel produced by a cell-traction mechanism in highly swollen collagenous gel, according to the method previously described,[13] was used as the hybrid tissue. Liver tissues of 6-week-old Wistar rats were used as *in vivo* models. Regardless of the tissue's being hybrid or living, the styrene-derivatized gelatin solution premixed with rhodamine-albumin was coated on the tissue surface and subsequently irradiated with visible-light to form a gel. Slices of a 3-day-cultured hybrid tissue also were subjected to fluorescence measurement. Three days after implantation, the liver tissue with the gel was harvested, fixed with 10% formalin neutral buffer solution (pH 7.4), dehydrated in a graded ethanol series, embedded in paraffin, and sectioned. After they were stained with hematoxylin-eosin, liver specimens were evaluated by light microscopy (AH-2 microscope, Olympus, Tokyo, Japan). The transverse slices, prepared with a micro-

slicer (VT-1000S, Leica, Nussloch, Germany), were observed by fluorescence microscopy (Eclipse E 800, Nikon, Tokyo, Japan).

RESULTS

Multiple styrene-derivatized gelatin was polymerized in the presence of a visible-light-induced radical-generating radical initiator to form a water-swollen gel. Various properties and performances of the gel required for *in situ* hydrogelation and its drug-releasing characteristics were determined according to material, formulation, and operation variables, listed in Figure 3.

Preparation of styrene-derivatized gelatin

According to the method previously described,[11] multiple styrene-derivatized gelatins with different degrees of derivatization [DD; defined as the percentage of derivatized residues relative to the total number of lysine residues (36.8 per molecule)] were prepared by a coupling reaction of the amino groups of the lysine residues of gelatin (MW: 9.5×10^4) with 4-vinylbenzoic acid in the presence of water-soluble carbodiimide (WSC) as a condensation agent in water. Extensive dialysis, followed by freeze-drying, produced a white powdery substance. All styrene-derivatized gelatins were soluble in water. Different DDs ranging from 10 to 78% were obtained under a fixed WSC concentration and reaction time but with different concentrations of 4-vinylbenzoic acid. As shown in Figure 4, DD was directly proportional to the initial feed concentration of 4-vinylbenzoic acid under the present experimental conditions.

Photocuring characteristics

Vigorous mixing of styrene-derivatized gelatin and carboxylated camphorquinone in PBS, followed by degassing, produced a viscous homogeneous solution. Visible-light irradiation resulted in gel formation. The gel yield and the degree of swelling (DS) in water varied with changes in formulation parameters, such as DD, gelatin concentration, and initiator concentration, and in operation parameters, such as photoirradiation time, as will be described below.

Figure 5(A) shows the effects of irradiation time on gel yield under fixed conditions (gelatin concentration, CQ concentration) but different DDs. Irrespective

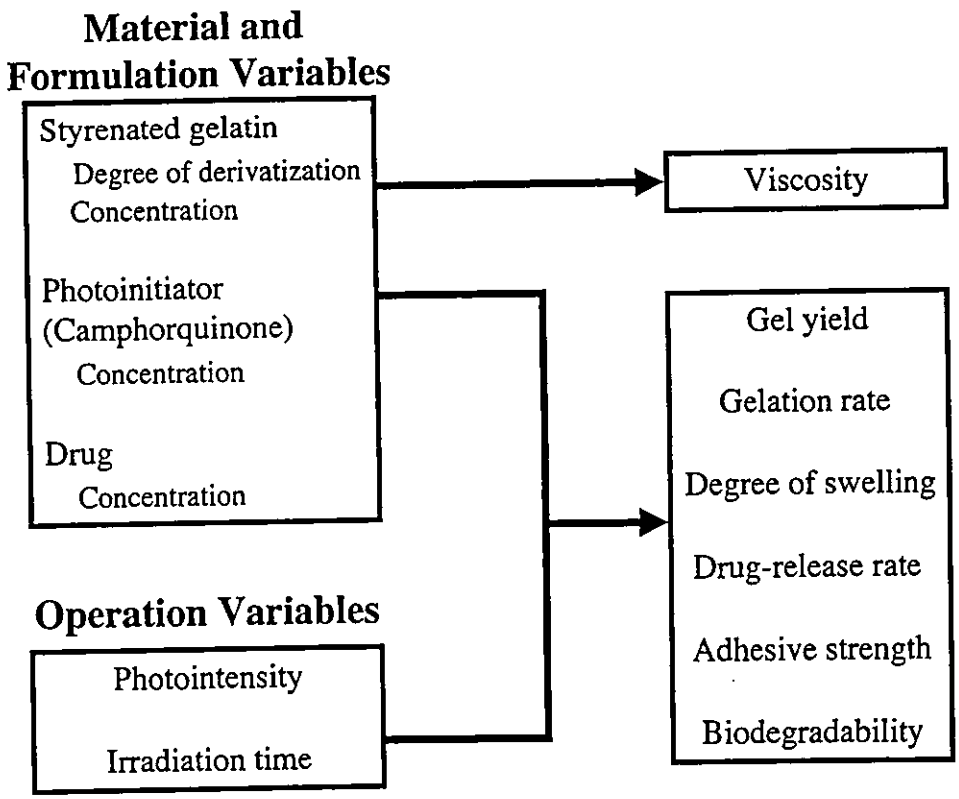

Figure 3. Inter-relationships among material variables, formulation variables, and operation variables with performances/properties.

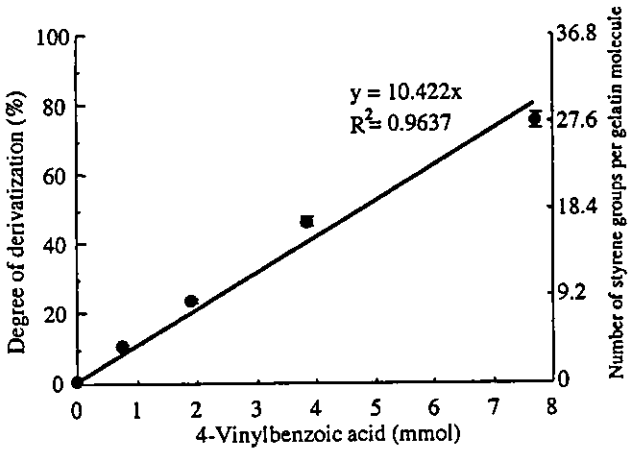

Figure 4. Degrees of derivatization of styrene groups into gelatin molecule by condensation of gelatin with different concentrations of 4-vinylbenzoic acid (n = 3). Values are expressed as means ± SD.

of DD, gelatin solutions solidified to form a gel within 1 min of irradiation. The gel yield increased with an increase in irradiation time of up to 3 min.

The resultant gels, which were prepared from gelatins with different DDs and subjected to different irradiation times, exhibited different DSs (Fig. 5(B)). DS decreased as the irradiation time increased, but little decrease in DS was observed after more than 3 min of irradiation.

Figure 6(A) shows the effect of CQ concentration on gel yield under fixed conditions (styrene-derivatized gelatin: DD, 78%; concentration, 30 wt %; and irradiation time, 3 min). Gel yield increased with an increase in CQ concentration up to 0.05 wt % and then leveled off above this concentration. Figure 6(B) shows the effect of CQ concentration on DS of photocured gels. DS decreased as CQ concentration was increased.

The dependence on gelatin concentration of gel yield as well as DS is shown in Figure 7. The increases in gelatin concentration and in DD resulted in an increase in gel yield and a concomitant decrease in DS of the formed gels.

The surface structure of the photocured gels was observed microscopically by SEM after freeze-drying. Figure 8 shows that the gelatin fibers were randomly crosslinked to form a gel. The network mesh formed using gelatin with a low DD (24%) appeared to be coarser than that formed using gelatin with a high DD (78%).

Drug release behavior

Rhodamine-albumin as a model proteinaceous drug was mixed with a styrene-derivatized gelatinous solution containing CQ and subsequently photocured. The amount of dye-conjugated albumin that diffused out from the gel into PBS was determined at fixed time intervals using a spectrophotometer. Figure 9 shows the time-dependent change of the amount of fractional dye-conjugated albumin for various photocured gels prepared with different DDs and gelatin concentrations. Irrespective of DD and gelatin concentration, rhodamine-albumin was released from the gels with time. The release rate and the final fractional release achieved are very strongly dependent on DD and gelatin concentration.

In order to quantify this dependence, the apparent diffusion coefficient was calculated in a manner shown in Equation (3), which is based on the Fickian diffusion process.[12] The fractional release (M_t/M_∞) increased linearly with the square root of time at the early stage. Figure 10 shows the linear dependence of the early-time rhodamine-albumin release on $t^{1/2}/\delta$,

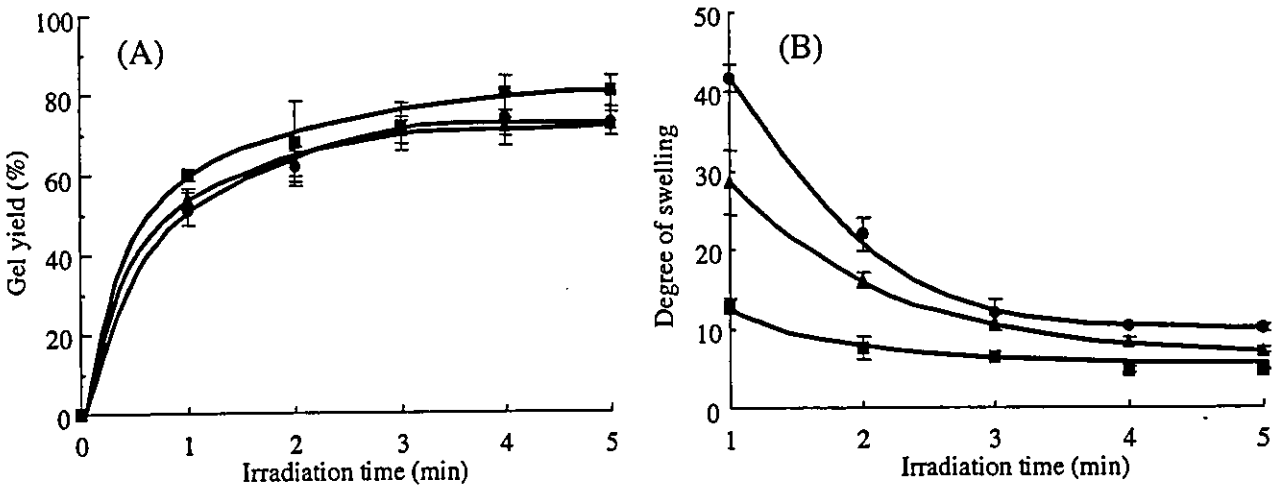

Figure 5. Effects of irradiation time and degree of derivatization on (A) gel yield and (B) degree of swelling. Gelatin concentration: 30 wt % [DD: 24% (●), 49% (▲), and 78% (■)]. The concentration of CQ was fixed at 0.05 wt % of the gelatin contained in the aqueous gelatin solution (n = 3). Values are expressed as means ± SD.

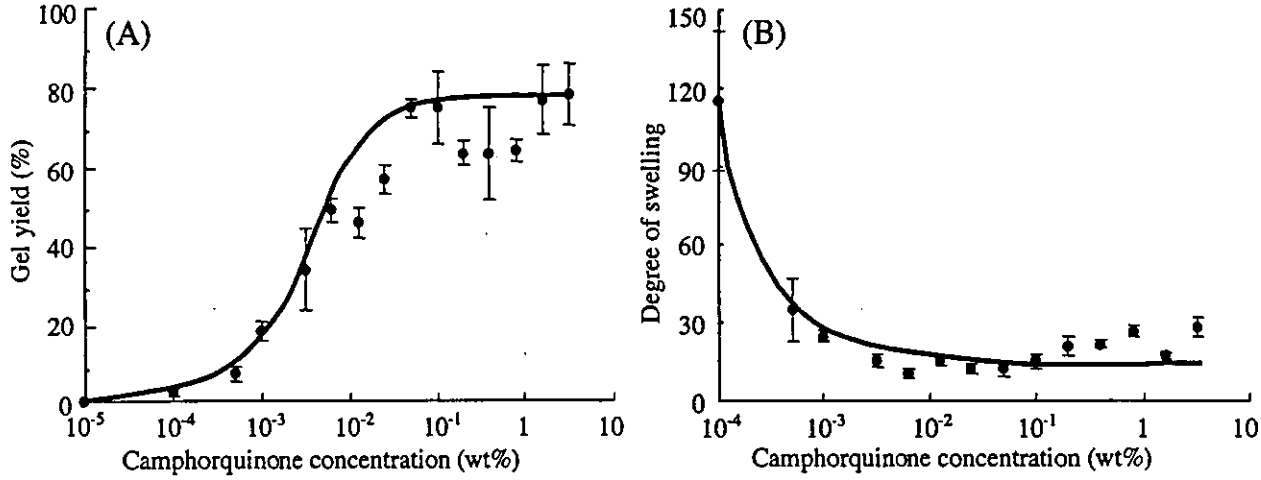

Figure 6. Effects of CQ concentration on (A) gel yield and (B) degree of swelling. Aqueous gelatin solution containing 30 wt % of styrene-derivatized gelatin (DD: 78%) was exposed for 3 min to 1.3×10^6 lx of visible-light irradiation ($n = 3$). Values are expressed as means ± SD.

based on a Fickian analysis. The dependence of the diffusion coefficient on gelatin concentration is shown in Figure 11(A). Apparently, the diffusion coefficient progressively decreased as both gelatin concentration and DD increased. The dependence on DS of the diffusion coefficient is shown in Figure 11(B). Other than that of rhodamine-albumin (MW: 6.6×10^4), the release of other rhodamine-conjugated proteins with different molecular weights, such as lactalbumin (MW: 1.4×10^4) and IgG (MW: 1.6×10^5), from the gel (concentration of the gelatin: 20 wt %, DD: 24%) is measured and the results are shown in Figure 12. Irrespective of the species or molecular weight of proteins, little difference in release rate was observed.

Tissue adhesion

When applied to living tissues, as an *in situ* photogelation drug-incorporating matrix, the viscosity of the photoreactive gelatin solution and the tissue adhesiveness of the gel are both important. If viscosity is low, the applied solution flows away from the tissue, whereas if it is high, the contact with tissues will be hampered. Figure 13(A) shows the logarithm of the viscosity of gelatin solution plotted against the concentration of gelatin (DD: 78%) at 25° and at 37°C. Viscosity increased almost exponentially as gelatin concentration increased. Gelatin solutions with gelatin concentrations below 20 wt % were found to be too fluid whereas those with gelatin concentrations above 40 wt % were too viscous. The optimum working viscosity was found to be around 30 wt %.

Figure 13(B) shows the adhesive strength to a swollen collagen film as a model tissue. Although there appears to be a gelatin concentration that gives the maximum tissue adhesive strength for gelatins with high DDs, the trend is that higher gelatin concentration and higher DD result in higher adhesive strength. The maximal adhesive strength (157.1 ± 14.6 g/cm^2) obtained was higher than that of fibrin glue (45.2 ± 7.1 g/cm^2).

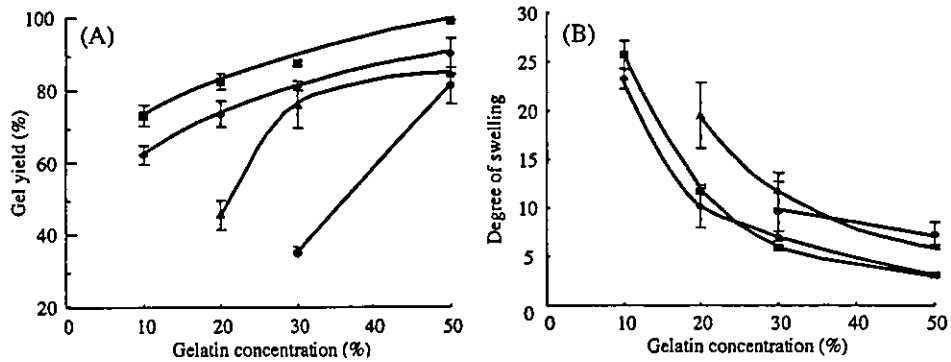

Figure 7. Effect of gelatin concentration on (A) gel yield and (B) degree of swelling. DD: 11% (●), 24% (▲), 49% (♦), and 78% (■). CQ concentration was fixed at 0.05 wt % of the gelatin contained in the aqueous gelatin solution. Visible-light irradiation was for 3 min at a photointensity of 1.3×10^6 lx ($n = 3$). Values are expressed as means ± SD.

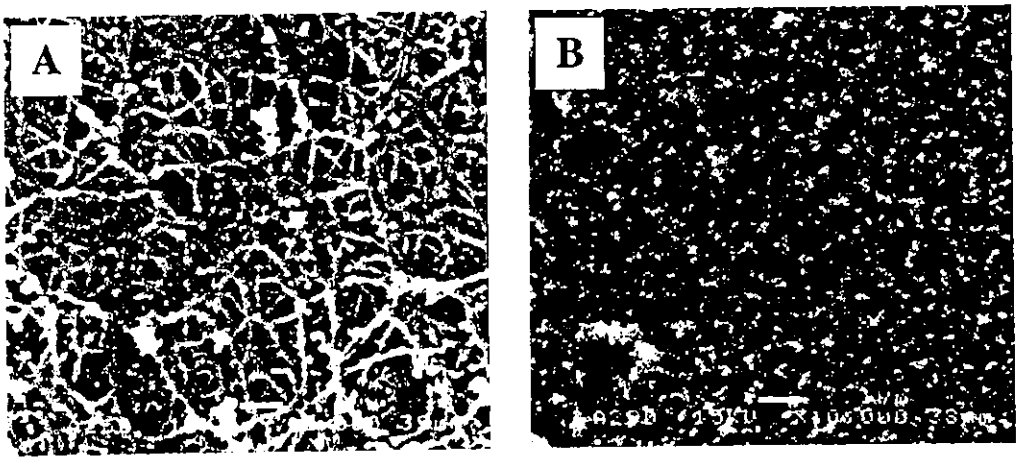

Figure 8. Scanning electron micrographs of the surface of gelatinous gel. Gelatin concentration: 30 wt %. (A) DD: 24%; (B) DD: 78%. Original magnification ×10,000. Bar represents 1 μm.

Tissue permeability

Prior to an extensive study focusing on *in situ* controlled release therapeutic efficacy on an experimental specific disease model *in vivo*, we conducted two preliminary *in vitro* and *in vivo* experiments. The *in vitro* experiment was conducted using a disk-type hybrid tissue that was a relatively dense tissue prepared from

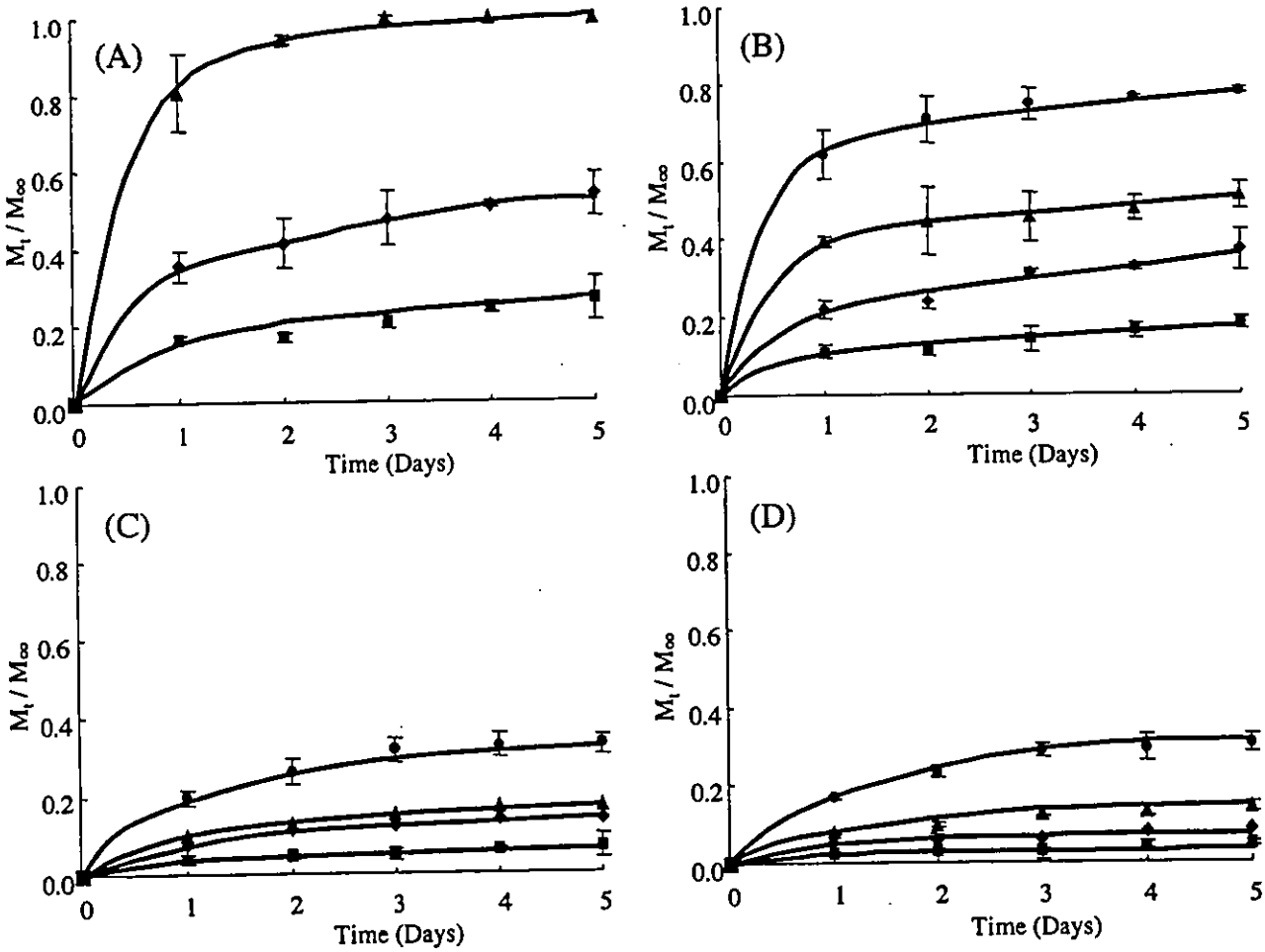

Figure 9. Fractional release of rhodamine-albumin from different systems, as a function of time. DD: (A) 11%; (B) 24%; (C) 49%; and (D) 78%. Gelatin concentration: 10 wt % (●); 20 wt % (▲); 30 wt % (♦); and 50 wt % (■). The concentration of CQ was fixed at 0.05 wt % of the gelatin contained in the aqueous gelatin solution. Visible-light irradiation was for 3 min at a photointensity of 130 × 10^4 lx. M_t is the amount released from the gel at any time, M_∞ is the total amount released at infinite time (n = 3). Values are expressed as means ± SD.

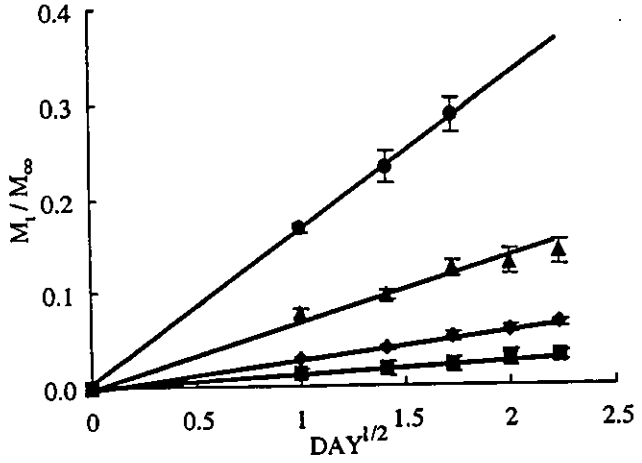

Figure 10. Short-time dependence of albumin release from the gel on $t^{1/2}$. DD: 78%. Gelatin concentration: 10 wt % (●); 20 wt % (▲); 30 wt % (♦); and 50 wt % (■) (n = 3). Values are expressed as means ± SD.

collagen and fibroblasts.[13] A rhodamine-albumin-containing thin-layered, photocured gelatin was formed on a tissue. Figure 14(A) shows the gel that was formed on the hybrid tissue. A fluorescence micrograph of the cross-sectional sliced tissue shows that albumin released from the gel permeated into the hybrid tissue [Fig. 14(B)].

Figure 15(A) shows the procedure of visible-light irradiation of the aqueous gelatin solution on the liver surface. Figure 15(B) shows that the gel was formed on the liver surface. Three days after implantation, the gel was found to adhere to the liver surface [Fig. 15(C)]. Histologic examination of the cross-sectional specimens stained with hematoxylin-eosin also confirmed that the gel tightly adhered to the tissue [Fig. 15(D)]. The fluorescence micrograph shows that rhodamine-albumin released from the gel permeated into the liver tissue [Fig. 15(E)].

DISCUSSION

It is possible that malignant tissues cannot be completely removed even by radical surgery. In such cases, highly effective chemotherapy that is conducted immediately after the removal of malignant tissues must be achieved by a locally sustained release of drugs directly into tissues where there may be remnant malignant cells. Our therapeutic strategy to this end involves immobilization of a drug *in situ* at the site where surgery for the removal of malignant tissue has been conducted. To realize this, we attempted to devise a local drug delivery technology that permits *in situ* drug loading, gelation, and tissue adhesion immediately after surgery together with sustained release of the drug and biodegradation of the drug-immobilized matrix over a period of time. As a basic matrix for *in situ* drug delivery, a tissue-adhesive material (gelatin) was employed.

Gelatin, a thermally denatured collagen,[14] has been used in a variety of biomedical applications, including drug-releasing matrices,[15,16] hemostatic aids or tissue adhesives,[10,11,17] and matrices or scaffolds for tissue-engineered devices.[18–20] Chemically crosslinked gelatins as release matrices in drug-delivery systems usually have been prepared using condensation agents such as N,N-(3-dimethylaminopropyl)-N'-ethyl carbodiimide (EDC)[21] or N-hydroxysuccinimide (NHS).[17] On such microporous gelatin foams fabricated by freeze-drying, drug loading usually is achieved by sorption of a drug-containing solution into these foams and subsequent drying.

On the other hand, the advantage of using photocuring or a photopolymerization technique is the superior temporal and spatial control of gelation that proceeds only when and where light is irradiated onto the photomerizing solution. Photopolymerization is a fast and efficient method of converting a solution into

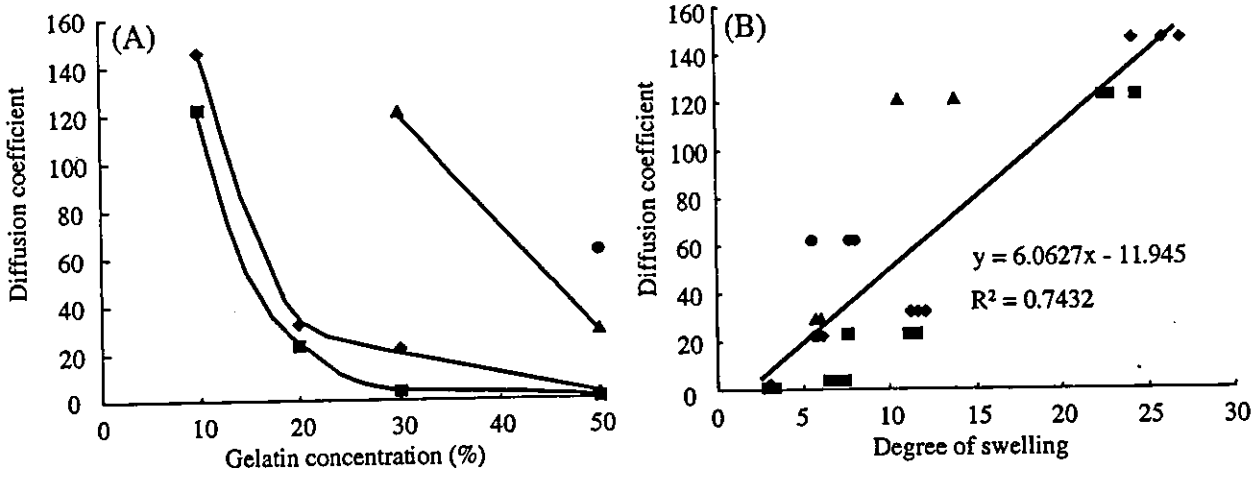

Figure 11. (A) Dependence of diffusion coefficient on gelatin concentration and DD. DD: 11% (●); 24% (▲); 49% (♦); and 78% (■). (B) Relationship between degree of swelling and diffusion coefficient. DD: 11% (●); 24% (▲); 49% (♦); and 78% (■).

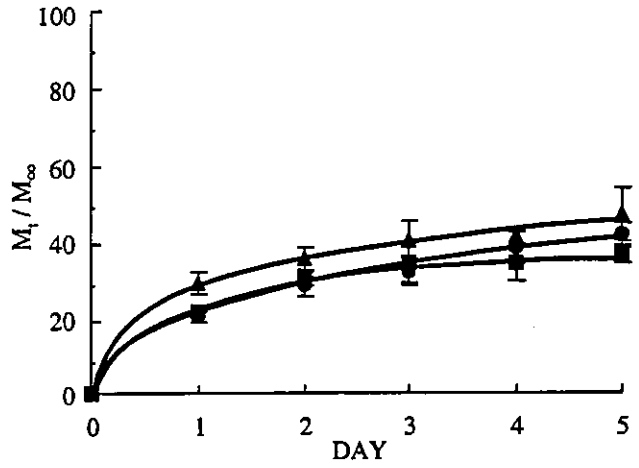

Figure 12. Release of rhodamine-conjugated proteins [alpha-lactalbumin (●), albumin (▲), and IgG (■)] from the gel over time. DD: 24%; gelatin concentration: 20 wt %. CQ concentration was fixed at 0.05 wt % of the gelatin contained in the aqueous gelatin solution. Visible-light irradiation was for 3 min at a photointensity of 1.3×10^6 lx ($n = 3$). Values are expressed as means ± SD.

gel *in situ* under ambient conditions. Other advantages include very easy, controllable manipulation of gelation characteristics, drug-releasing characteristics, and *in situ tissue adhesion, and also in situ* drug immobilization without substantial loss of precious bioactive substances. Such characteristics can be manipulated by material variables such as DD and gelatin concentration, formulation variables such as CQ concentration and drug concentration, and operation variables such as photointensity and irradiation time.

Figure 3 shows the inter-relationships among these variables and performances/properties. The combination of these variables determines the viscosity of the aqueous gelatin solution, gel yield, gelation rate, degree of swelling, drug-release rate, tissue adhesive strength, and biodegradability. Therefore, it can be said that a photochemically driven controlled-release system potentially possesses a wide variety of delivery characteristics, as listed above. The following is a summary of how these variables affect gelation and drug-release characteristics.

1. At low gelatin concentrations, higher DDs result in higher gel yields [Fig. 7(A)] whereas there is no appreciable dependence of DDs on gel yield at higher gelatin concentrations [e.g., over 30 wt %; Fig. 5(A)]. The higher the initiator concentration, the higher the gel yield [Fig. 6(A)]. On the other hand, the degree of swelling of the formed gels in water is dependent on both gelatin concentration and DD. Within a few minutes of irradiation, sol-to-gel phase transformation is achieved upon visible-light irradiation. The solution viscosity, which does not induce flow away from the living tissue, is dependent mainly on gelatin concentration [Fig. 13(A)]. This ease of handling is a great advantage for use in clinical application.
2. As for the release characteristics of rhodamine-albumin from gels into PBS, the release rate is dependent on gelatin concentration and DD; that is, the higher gelatin concentration and DD, the slower the release rate (Fig. 9). Since there is a linear dependence of the early fractional release on the square root of time (Fig. 10), the release characteristics in the early period obey the Fickian diffusion process expressed in Equation (3). The diffusion coefficient calculated using Equation (3) is markedly dependent on gelatin concentration and DD [Fig. 11(A)]. There is a rough

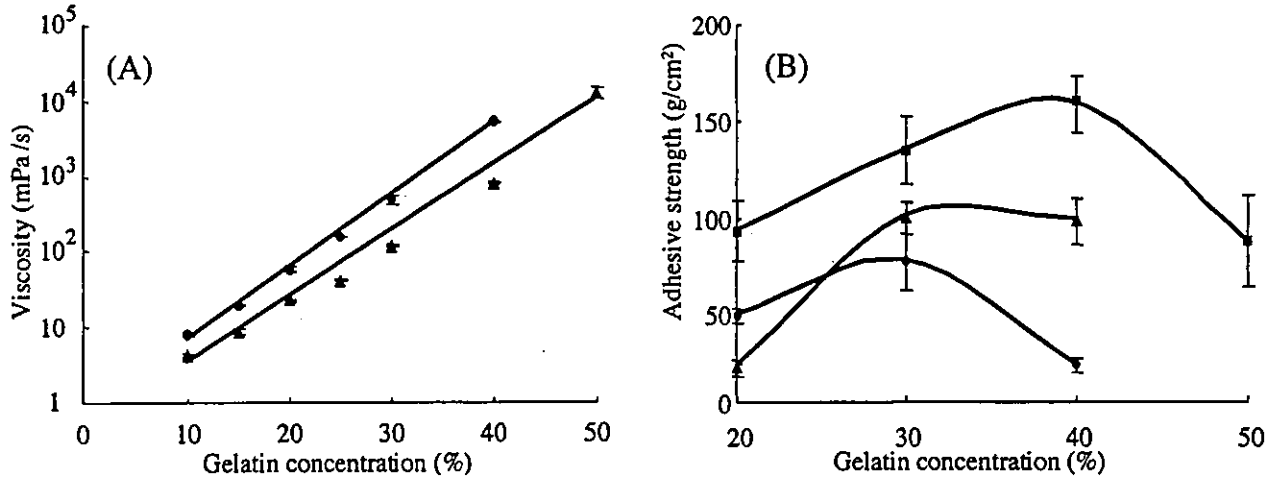

Figure 13. (A) Viscosity of aqueous gelatin solution with different concentrations of gelatin (DD: 78%) at 25°C (●) and 37°C (▲) ($n = 3$). Values are expressed as means ± SD. (B) Adhesive strength of wet collagen film. 100 μL of aqueous gelatin solution was poured onto the collagen film (diameter: 7 mm), and a photocurable gel was prepared by exposure for 3 min to 1.3×10^6 lx of visible-light irradiation. CQ concentration was fixed at 0.05 wt % of the gelatin contained in the aqueous gelatin solution. DD: 24% (●); 49% (▲); and 78% (■) ($n = 3$). Values are expressed as means ± SD.

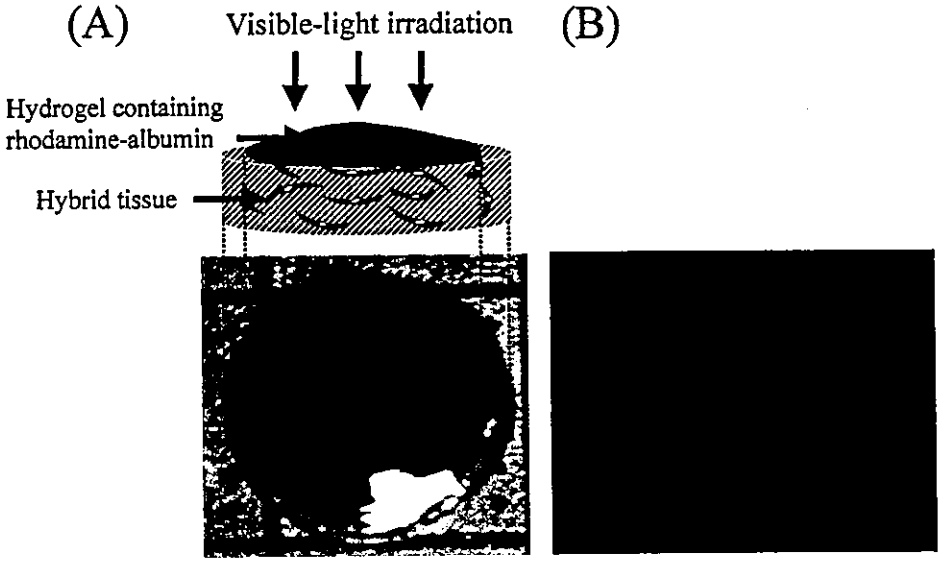

Figure 14. *In vitro* drug permeability in a disk-type hybrid tissue. (A) Gel formed on the hybrid tissue; (B) fluorescence micrograph of cross-sectional sliced tissue.

relationship between the diffusion coefficient and the degree of swelling, that is, the higher the degree of swelling, the higher the diffusion coefficient [Fig. 11(B)]. Therefore, the desired release rate of the gel is manipulated by controlling the degree of swelling, a key index of drug-release characteristics, by both DD and gelatin concentration. Although such *in vitro* drug-release characteristics do not necessarily reflect or predict those *in vivo* because of the biodegradation that

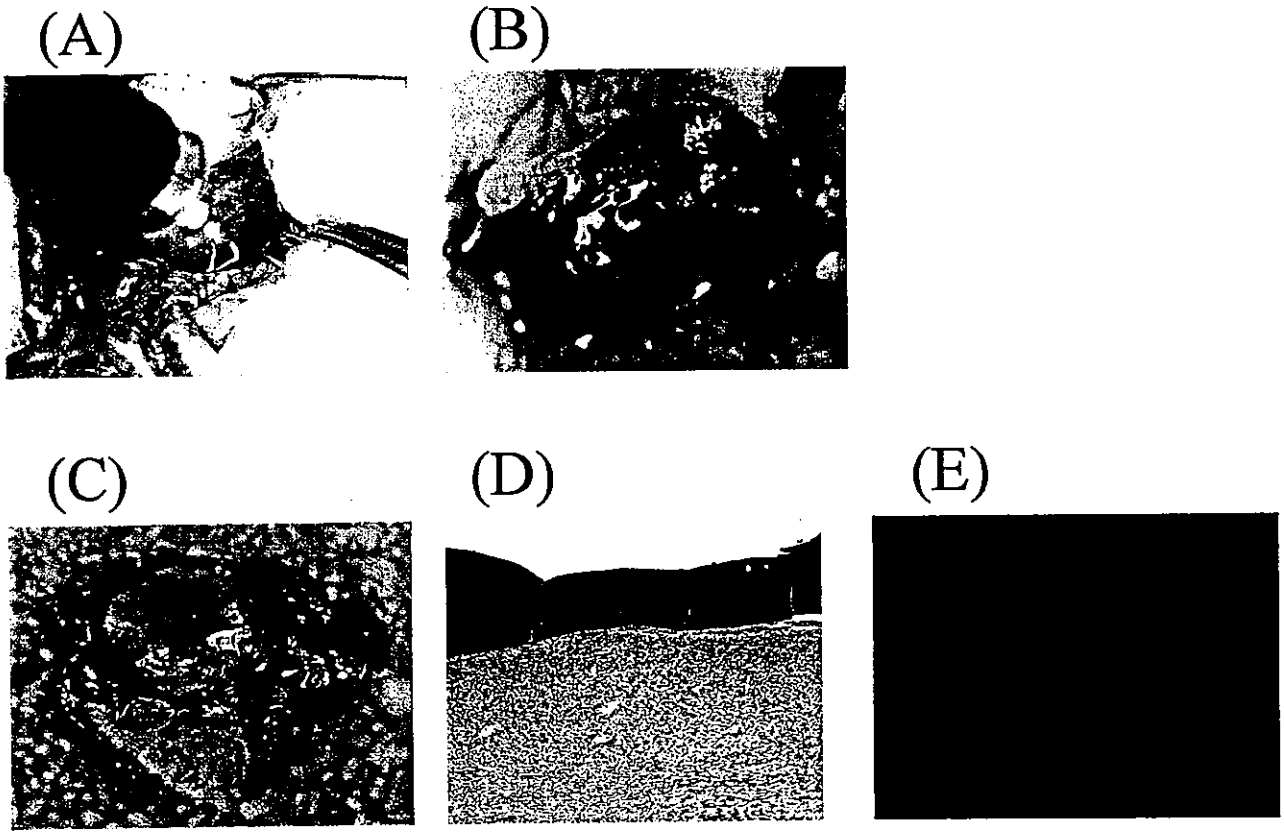

Figure 15. *In vivo* drug permeability in rat liver tissue. (A) Procedure of visible-light irradiation of the aqueous gelatin solution on the liver surface; (B) gel formed on the liver surface; (C) resected specimen (3 days after implantation); (D) cross-sectional specimen (HE staining); and (E) fluorescence micrograph of cross-sectional specimen.

occurs with implantation time and the type of tissue involved, manipulation of the drug-release characteristics on the order of days to months may be feasible. That is, short-term drug-release can be attained by the gelatinous system with low DD and low gelatin concentration whereas long-term sustained release can be achieved by the system with high DD and high gelatin concentration. Since the diffusion coefficient is reduced markedly as DD and gelatin concentration increase, a gelatinous structure with a small network mesh size, as evidenced by SEM observation, appears to retard drug release. In contrast, little difference in the release rate was observed when the molecular weights of drugs were changed. Since the drug-release characteristics obey Fick's second law of diffusion in the early period of release, the drug-release rate must be determined by the ratio of the drug radius to the network mesh size of gels. That is, a large-sized protein must have a low release rate if such a ratio is sufficiently high. In the case of a low ratio (i.e., high mesh size), the drug-size effect should be minimized. In fact, freeze-dried SEM samples of photocured gelatins show a fibrous mesh network, the size of which is much larger than those of the proteins used.

3. The *in vitro* study showed that the photocured gel adhered to the collagen film more tightly than fibrin glue. The adhesive strength of photocured gelatin (prepared using gelatin with DD of 78% at a gelatin concentration of 40 wt %) was about four times higher than that of the fibrin glue. At 1-month implantation, the cross-section of the specimen clearly showed that the gel tightly adhered to the rat liver surface (data not shown). The gel was biodegraded and biosorbed. Biodegradation is related to cellular infiltration and ingrowth into the gel due to a foreign-body reaction. Cellular ingrowth was observed at 1 week after implantation. At 4 weeks, full ingrowth of giant cells, lymphocytes, and fibroblasts was observed; the fibrous tissue, which was more prominent, showed higher vascularization with more macrophages than it did at 2 weeks (data not shown). Since the *in vivo* degradation rate of gel can be controlled by the density of gel and the crosslinking density, it is considered that the degradation period from 1 to several months may be attained, which depends on the formulation of the gel.

Since photocurable gelatin is modified minimally by the introduction of styrene groups, it is possible that it is nontoxic in nature. In addition, visible-light irradiation itself does not induce any substantial damage at cell and tissue levels (We used a light apparatus that has been used in dental treatment). However, the potential hazard derived from radicals generated by camphorquinone, which also is an active ingredient for photocurable dental resin,[22] upon visible-light irradiation cannot be completely ruled out. However, the CQ concentration used in this system is less than 0.01~0.02 wt % of the photoreactive solution. It is suspected that spontaneous cell damage due to radicals may be minimal in this application.[23] In fact, *in situ* gelation on rat liver surface induced neither degeneration nor necrosis of the hepatocytes (data not shown).

As a therapeutic application of this technology, we strongly believe that this *in situ* photocuring drug-release system should be used in the postoperative treatment of carcinogenic tissues. The *in situ* photoconstruction of a local drug-delivery system would allow surgeons to minimize tumor recurrence via highly localized drug delivery through a layering onto tissues or direct injection into them, as shown in Figure 1. Irrespective of the "on-tissue" or "in-tissue" method, compared with ultraviolet-light-driven procedures and chemical-based methods, the visible-light-photocuring method developed here is only minimally harmful to living cells.

In cancer chemotherapy, the strategy of "cytostasis" instead of "cytokilling" is in the mainstream because conventional chemotherapy has reached its limits. Recently, various bioactive substances for tumor dormancy therapy have been developed for this purpose. These proteinaceous drugs include angiostatin (MW: 3.8×10^4),[24] endostatin (MW: 2.0×10^4),[25] and HGF/NK4 [MW: 6.7×10^4; an antagonist for the hepatocyte growth factor (HGF)],[26] which have functions of inhibiting tumor growth, metastasis, and angiogenesis. Our ongoing investigation, aimed at the development of a therapeutic procedure, will focus on immobilizing HGF/NK4 in gelatinous hydrogel for preventing the recurrence of tumors, particularly pancreatic cancer.

CONCLUSIONS

In order to prevent tumor recurrence, we devised an *in situ* processable tissue-adhesive localized drug-release system, to be utilized immediately after the removal of malignant tissues. This *in situ* gelation technology may be effective in inhibiting tumor recurrence. Extensive *in vitro* studies using hybrid tissues and *in vivo* studies are ongoing, the results of which will be reported in the near future.

The authors thank Dr. Toshinobu Sajiki for technical support and Kanna Okuda for viscosity measurements.

References

1. Colter KD, Bell AT, Shen M. Control of the pilocarpine release rate through hydrogels by plasma treatment. Biomater Med Devices Artif Org 1977;5:1–12.

2. Atkins TW, McCallion RL, Tighe BJ. The incorporation and sustained release of bioactive insulin from a bead-formed macroporous hydrogel matrix. J Biomed Mater Res 1995;29:291–298.
3. Lyman MD, Melanson D, Sawhney AS. Characterization of the formation of interfacially photopolymerized thin hydrogels in contact with arterial tissue. Biomaterials 1996;17:359–364.
4. Hill-West JL, Chowdhury SM, Sawhney AS, Pathak CP, Dunn RC, Hubbell JA. Prevention of postoperative adhesions in the rat by in situ photopolymerization of bioresorbable hydrogel barriers. Obstet Gynecol 1994;83:59–64.
5. Cruise GM, Hegre OD, Lamberti FV, Hager SR, Hill R, Scharp DS, Hubbell JA. In vitro and in vivo performance of porcine islets encapsulated in interfacially photopolymerized poly(ethylene glycol) diacrylate membranes. Cell Transplant 1999; 8: 293–306.
6. Elisseeff J, McIntosh W, Anseth K, Riley S, Ragan P, Langer R. Photoencapsulation of chondrocytes in poly(ethylene oxide)-based semi-interpenetrating networks. J Biomed Mater Res 2000;51:164–171.
7. Sawhney AS, Pathak CP, Hubbell JA. Interfacial photopolymerization of poly(ethylene glycol)-based hydrogels upon alginate-poly(l-lysine) microcapsules for enhanced biocompatibility. Biomaterials 1993;14:1008–1016.
8. Kim SH, Chu CC. In vitro release behavior of dextran-methacrylate hydrogels using doxorubicin and other model compounds. J Biomater Appl 2000;15:23–46.
9. Scott RA, Peppas NA. Highly crosslinked, PEG-containing copolymers for sustained solute delivery. Biomaterials 1999;20: 1371–1380.
10. Nakayama Y, Matsuda T. Newly designed hemostatic technology based on photocurable gelatin. Am Soc Artif Intern Org J 1995;41:374–378.
11. Nakayama Y, Matsuda T. Photocurable surgical tissue adhesive glues composed of photoreactive gelatin and poly(ethylene glycol) diacrylate. J Biomed Mater Res 1999;48:511–521.
12. J. Crank. The Mathematics of diffusion. Oxford: Oxford University Press; 1956.
13. Okano T, Matsuda T. Hybrid muscular tissues: Preparation of skeletal muscle cell-incorporated collagen gels. Cell Transplant 1997;6:109–118.
14. Rose PI. Gelatin. In: Mark HF, Bikales NM, Overberger CG, Menges G, Kroschwitz JI, editors. Encyclopedia of polymer science and engineering. New York: Wiley; 1987. p 488–513.
15. Bozzay J, David A, Denes M, Rusznak I. Production of granules with controlled drug release rate. Pharmazie 1979;34:172–174.
16. Yamamoto M, Tabata Y, Hong L, Miyamoto S, Hashimoto N, Ikada Y. Bone regeneration by transforming growth factor beta1 released from a biodegradable hydrogel. J Controlled Release 2000;64:133–142.
17. Iwata H, Matsuda S, Mitsuhashi K, Itoh E, Ikada Y. A novel surgical glue composed of gelatin and N-hydroxysuccinimide activated poly(L-glutamic acid). I. Synthesis of activated poly(L-glutamic acid) and its gelation with gelatin. Biomaterials 1998;19:1869–1876.
18. McDonald JA, Kelley DG, Broekelmann TJ. Role of fibronectin in collagen deposition: Fab' to the gelatin-binding domain of fibronectin inhibits both fibronectin and collagen organization in fibroblast extracellular matrix. J Cell Biol 1982;92:485–492.
19. Thomson RC, Yaszemski MJ, Powers JM, Mikos AG. Fabrication of biodegradable polymer scaffolds to engineer trabecular bone. J Biomater Sci, Polym Edn 1995;7:23–38.
20. Choi YS, Hong SR, Lee YM, Song KW, Park MH, Nam YS. Studies on gelatin-containing artificial skin. II. Preparation and characterization of crosslinked gelatin–hyaluronate sponge. J Biomed Mater Res 1999;48:631–639.
21. Ofner CM 3rd, Bubnis WA. Chemical and swelling evaluations of amino group crosslinking in gelatin and modified gelatin matrices. Pharm Res 1996;13:1821–1827.
22. Nakazato J, Itoh K, Wakumoto S. Light activated resin containing organic dyestuff. Dent Mater J 1989;8:147–154.
23. Bryant SJ, Nuttelman CR, Anseth KS. Cytocompatibility of UV and visible light photoinitiating systems on cultured NIH/3T3 fibroblasts in vitro. J Biomater Sci, Polym Edn 2000;11:439–457.
24. O'Reilly MS, Holmgren L, Shing Y, Chen C, Rosenthal RA, Moses M, Lane WS, Cao Y, Sage EH, Folkman J. Angiostatin: A novel angiogenesis inhibitor that mediates the suppression of metastases by a Lewis lung carcinoma. Cell 1994;79:315–328.
25. O'Reilly MS, Boehm T, Shing Y, Fukai N, Vasios G, Lane WS, Flynn E, Birkhead JR, Olsen BR, Folkman J. Endostatin: An endogenous inhibitor of angiogenesis and tumor growth. Cell 1997;88:277–285.
26. Date K, Matsumoto K, Shimura H, Tanaka M, Nakamura T. HGF/NK4 is a specific antagonist for pleiotrophic actions of hepatocyte growth factor. FEBS Lett. 1997;420:1–6.

ELSEVIER

Cardiovascular Research 53 (2002) 481–486

Cardiovascular Research

www.elsevier.com/locate/cardiores

Local delivery of low-dose docetaxel, a novel microtubule polymerizing agent, reduces neointimal hyperplasia in a balloon-injured rabbit iliac artery model

Satoshi Yasuda[a,*], Teruo Noguchi[a], Masahiro Gohda[a], Takashi Arai[b], Nobumasa Tsutsui[b], Yasuhide Nakayama[c], Takehisa Matsuda[c], Hiroshi Nonogi[a]

[a]*National Cardiovascular Center, Division of Cardiology, Department of Medicine, 5-7-1 Fujishiro-dai, Suita, Osaka 565-8565, Japan*
[b]*Tokai Medical Products Inc. Aichi, Japan*
[c]*National Cardiovascular Center Research Institute, Department of Bioengineering, Osaka, Japan*

Received 21 June 2001; accepted 4 October 2001

Abstract

Objective: Docetaxel (DOC) is a novel microtubule polymerizing agent, with superior antiproliferative properties as compared to paclitaxel. DOC is therefore a potential therapeutic tool for the prevention of restenosis following angioplasty. However, DOC has systemic toxicity such as leukocytopenia, which occurs in a dose-dependent manner. To minimize such adverse effects, we carried out local delivery of low-dose DOC directly to injured vessel sites. **Methods:** The rabbit iliac artery was denuded, and then DOC (2 mg) or control vehicle was administered locally 20 min, via a local drug delivery catheter. **Results:** The levels of DOC in the plasma were within ng/ml range, eliminating hematopoietic side effects. Seven days after the local delivery (DOC: $n=4$, control: $n=4$), DOC decreased the number of Ki-67-labeled cells in the intima (DOC: 22±10 vs. control: 66±18 cells/mm^2, $P<0.01$), indicating a decreased proliferative activity. At 28 days (DOC: $n=8$, control: $n=8$), computer-assisted morphometric analysis demonstrated that DOC significantly reduced the intimal area (DOC: 0.15±0.13 vs. control: 0.70±0.13 mm^2, $P<0.01$). There was also a decrease in medial area in the DOC-treated vessels (DOC: 0.62±0.17 vs. control: 1.13±0.38 mm^2, $P<0.01$). **Conclusions:** Local delivery of DOC, even after a single low-dose administration, effectively inhibits neointimal hyperplasia. Such administration is associated with a minimal likelihood of systemic adverse effects (leukocytopenia), but potentially induces local toxicity (a decrease in medial wall thickness) due to extensive cytotoxic effect.

Keywords: Angioplasty; Atherosclerosis; Pharmacokinetics; Histo(patho)logy; Restenosis; Smooth muscle

This article is referred to in the Editorial by M. Sturek and H.K. Reddy (pages 292–293) in this issue.

1. Introduction

Despite extensive effort, including the development of adjunctive therapies and mechanical techniques, 30–50% of patients, undergoing percutaneous transluminal coronary angioplasty (PTCA) develop restenosis within 3 to 6 months of the procedure [1]. In addition to vascular remodeling, neointimal hyperplasia is a major cause of restenosis in response to arterial injury [2]. This process predominantly involves vascular smooth muscle cell proliferation. Therefore, one of the therapeutic strategies for the prevention of restenosis is the suppression of such proliferation using cytostatic or cytotoxic agents [3].

Recent studies have revealed that the microtubules within cells are among the most important components of cellular dynamics, including mitosis, cell signaling and

Abbreviations: DOC=Docetaxel; PTCA=Percutaneous Transluminal Coronary Angioplasty; WBC=White Blood Cell; vWF=von Willebrand's factor

*Corresponding author. Tel.: +81-6-6833-5012; fax: +81-6-6872-7486.
E-mail address: syasuda@hsp.ncvc.go.jp (S. Yasuda).

Time for primary review 32 days.

0008-6363/02/$ – see front matter
PII: S0008-6363(01)00499-0

motility [4]. Microtubule polymerizing agents of taxoids, such as paclitaxel, inhibit cell proliferation by blocking mitosis, and are therefore currently used as anticancer drugs [5–7]. In vitro studies have shown that paclitaxel also inhibits vascular smooth muscle cell proliferation [8,9], indicating its potential therapeutic value against restenosis following PTCA.

Docetaxel (DOC: Taxotere®, Rhone Poulenc Rorer, Paris, France) is an analog of paclitaxel (*N*-debenzoyl-*N*-tert-butoxycarbonyl-10-deacetyl taxel) that more efficiently induces microtubule polymerization, with superior anticancer and antiproliferative properties as compared to paclitaxel [10,11]. The principal toxicity of DOC is leukocytopenia, which occurs in a dose-dependent manner. To minimize the likelihood of such systemic adverse effects, local administration of the drug directly to the target site has been attracting increasing interest [12]. In the previous studies [9,13], paclitaxel did not inhibit neointimal formation in rabbits after balloon injury. Therefore, in the present study, we tested our hypothesis that local delivery of a low dose of DOC, a novel and potent microtubule polymerizing agent, may attenuate the proliferative response to vascular injury, with reduced risk of systemic toxicity.

2. Methods

All the procedures were in accordance with the institutional guidelines, which conform to the 'Position of the American Heart Association on Research Animal Use'.

2.1. The model

New Zealand white rabbits weighing 3.0–3.5 kg were used for this study as in our previous one [14]. Anesthesia was induced by intramuscular injection of ketamine (50 mg/kg), following treatment with xylazine (10 mg/kg). The femoral arteries were exposed by an incision below the inguinal ligament. Heparin sulfate (1000 U) was administered intravenously to prevent blood coagulation. After administration of 2 ml of 1% lidocaine, a 3.6 Fr angioplasty catheter (Tokai Medical Products Inc., Aichi, Japan) [15] was introduced under fluoroscopic guidance by an over-the-wire system into the right iliac artery. This catheter [15] possesses the triple functions of balloon inflation, local administration and blood perfusion. This device was found to maintain 34±7 ml/min of distal blood flow during drug administration at a mean aortic pressure of 100 mm Hg in our pilot studies [15]. Thus, this device enables a drug delivery over a relatively long duration (20 min) with maintaining perfusion. As reported previously [14], the 3.0-mm-diameter balloon, 20 mm in length, was inflated with contrast medium at the right iliac artery immediately distal to the aortic bifurcation (a reliable and reproducible landmark for the removal of the vessels at a later date). The balloon inflated at 6 atm was then retracted and deflated. This procedure was repeated three times in the same segment (20 mm in length from the bifurcation) to ensure complete endothelial denudation.

2.2. Local delivery of docetaxel

Following the balloon-induced injury, local drug delivery was effected via a multifunctional angioplasty catheter. A detailed description of this device appears in our previous reports [14,15]. Briefly, the drug delivery port was positioned at the injured site and the balloon was inflated at a low pressure (2 atm) to allow accumulation of the drug. Then the guidewire was removed to a site proximal to the perfusion port to allow distal perfusion. In pilot studies using this device, the drug permeated into the medial and the adventitial tissues immediately after the delivery, and then persists in the medial tissue for at least 24 h. In addition, this device could deliver the drug homogeneously over 80% of the target site. Via an infusion pump (STC-521, Terumo, Japan), the rabbits were locally administered 2 mg of DOC dissolved in 10 ml saline (DOC group, $n=12$) or vehicle solution without DOC (Control group, $n=12$) over 20 min, via the local drug delivery catheter. The dose of DOC used in the present study (2 mg) was one order of magnitude lower than the dose of paclitaxel (~35 mg) used in the previous study in rabbits [9,13].

In the DOC group ($n=4$), blood samples were obtained 30 min after the drug administration and stored at −20°C. The DOC concentrations in the plasma were then measured at Mitsubishi Chemical BCL (Tokyo, Japan) by high-performance liquid chromatography, as described previously [16]. The concentration range was confirmed to be from 20 to 4000 ng/ml in the plasma [16].

2.3. White blood cell counting

DOC has systemic toxicity such as leukocytopenia, which occurs in a dose-dependent manner. To evaluate the hematopoietic effects of low doses of DOC, the white blood cell (WBC) number was counted in the DOC group ($n=4$). Blood samples were obtained before, 1, 3, 7, 14 and 28 days after the administration of DOC.

2.4. Postmortem procedures

Seven or 28 days after the procedure, the rabbits were sacrificed by injection of a fatal dose of pentobarbital. For pressure perfusion fixation, a mid-abdominal incision was made and the lower abdominal aorta was isolated, flushed with saline, and fixed with 10% buffered formalin at 80 mm Hg for over 15 min. At least 24 h postfixation, the arterial segments were dehydrated and embedded in paraffin [14].

2.5. Immunohistochemical analysis

In addition, to quantify the degree of smooth muscle cell proliferation, Ki-67 was immunohistochemically stained [17] in tissue specimens obtained 7 days after the drug administration. The primary antibody used was MIB-1 monoclonal antibody (DAKO, Denmark) [17]. The fraction of Ki-67-positive cells per mm^2 of the intimal layers was subsequently determined in the control (n=4) and DOC-treated vessels (n=4). Monocytes/macrophages were detected with monoclonal antibody against CD68 (DAKO). Arterial cross sections were also immunostained with primary antibody for von Willebrand's factor (vWF) (DAKO) as a marker for endothelial cells.

2.6. Morphometric analysis

For histology, 5-μm sections were cut and stained with elastic van Gieson or hemotoxylin–eosin. Morphometric analysis was performed on arterial cross sections at 28 days, and imaged using a National Institutes of Health image software package. The endoluminal border, the circumference bounded by the internal elastic lamina, and the external elastic lamina were manually traced, and then the luminal, intimal, and medial areas were calculated. Nuclear counts were also made in the media and intimal area. We compared these parameters between the control (n=8) and the DOC-treated vessels (n=8).

2.7. Statistics

All data were expressed as means±S.D. To compare the DOC group with the Control group, data were analyzed by the unpaired Student's t-test to evaluate the two-tailed levels. In the DOC group, the WBC data were compared by analysis of variance. A value of $P<0.05$ was considered as denoting significance.

3. Results

Even 0.5 h after the local administration, the plasma levels of DOC did not exceed 203±80 ng/ml (range of 114 to 270 ng/ml). Fig. 1 shows the serial changes in the WBC counts. There were no significant changes, indicating that the local delivery of a low dose of DOC is associated with minimal risk of leukocytopenia.

The degree of cell proliferation and the cell type were determined based on immunohistochemical studies (Fig. 2). At 7 days, the number of cells positive for vWF (against endothelial cells) and CD-68 (against macrophages) were not significantly different between the two groups. However, the number of Ki-67-positive cells was

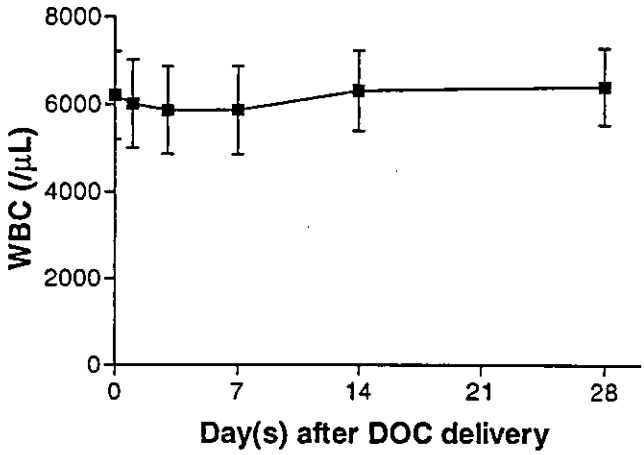

Fig. 1. Serial changes in means±S.D. data of white blood cell (WBC) count after local delivery of DOC (n=4).

22±10 cells/mm^2 in the DOC group, significantly lower than the number, 66±18 cells/mm^2 ($P<0.01$), in the Control group. This finding suggests a decreased proliferative activity of vascular smooth muscle cells in the vessels administered with DOC.

Fig. 3 shows representative photomicrographs of histologic cross sections from the injured arterial segments at 28 days. Table 1 summarizes the group morphometric data 28 days after the administration. Local delivery of 2 mg DOC induced a significant reduction in the intimal area, and a decrease in the intima-to-media area ratio. Although these findings indicate suppression of neointimal hyperplasia by the microtubule polymerizing agent, there was also a decrease in medial area in the DOC-treated vessels. The cell density in the media was significantly lower in the DOC group than in the Control group (650±102 vs. 819±124 counts/mm^2, $P<0.01$).

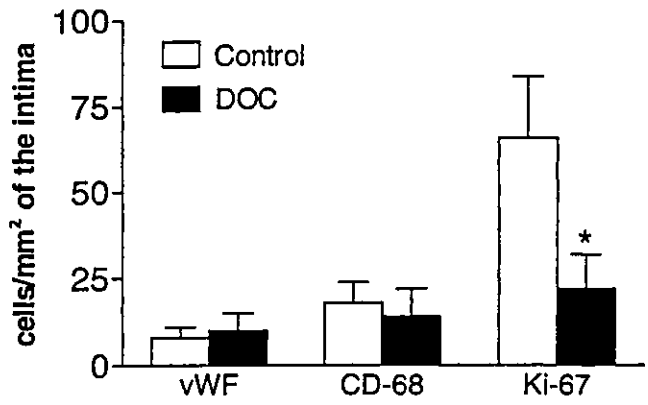

Fig. 2. Quantitative immunohistochemical examinations at 7 days in the Control (untreated-) vessels (open bars: n=4) and Docetaxel (DOC)-treated vessels (closed bars: n=4). The means±S.D. data of the number of cells positive for von Willebrand's factor (vWF) (against endothelial cells), CD-68 (against macrophages), and Ki-67, respectively, are shown. * $P<0.05$ vs. control by unpaired t-test.

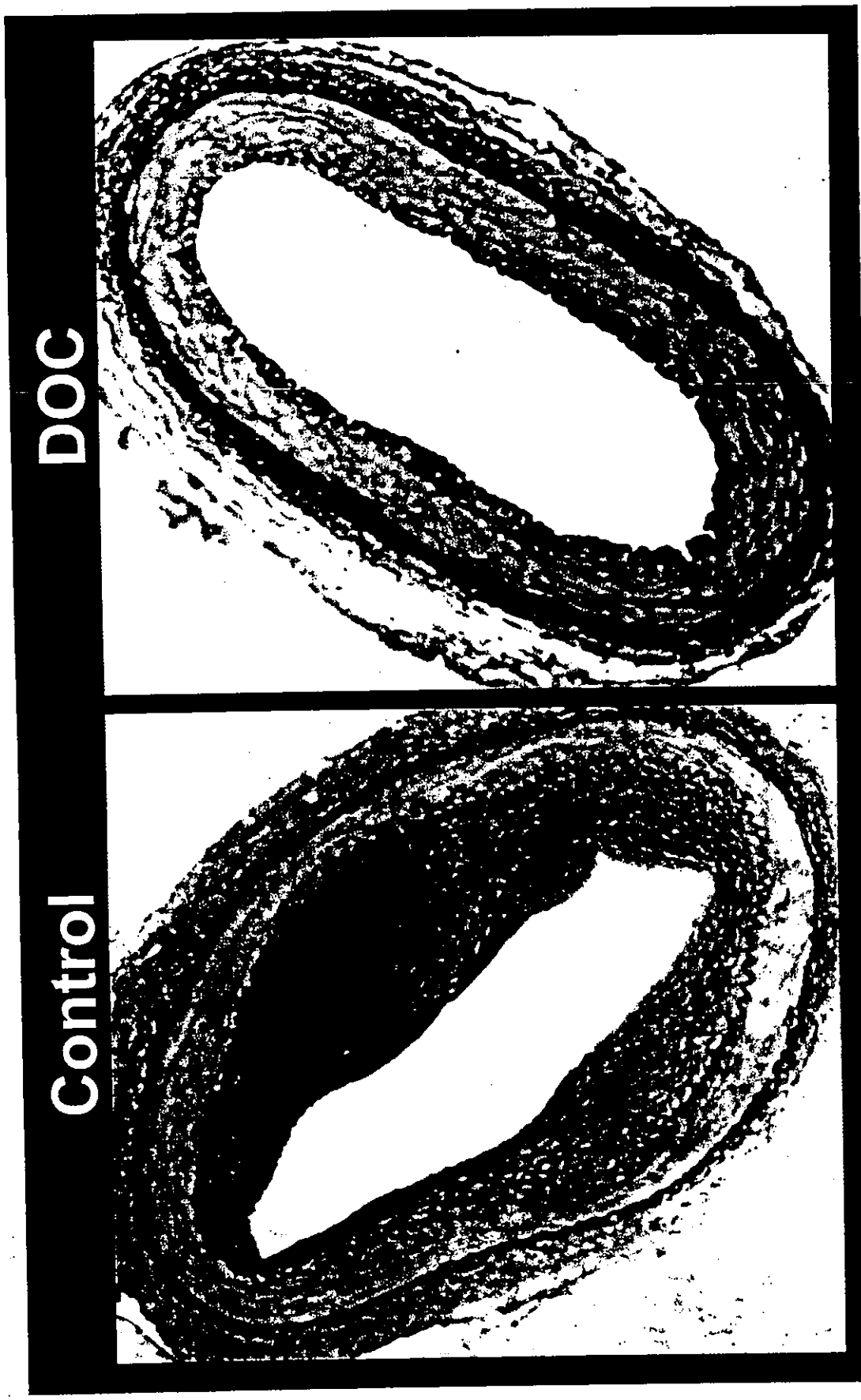

Fig. 3. Cross section (elastin van Gieson stain) of rabbit iliac arteries 28 days after balloon-induced injury. Left panel: Control (untreated-) artery (×40). Right panel: DOC-treated artery (×40). Note marked reduction in intimal hyperplasia in DOC-treated artery.

Table 1
Comparison of arterial morphomeric data 28 days after the local administration of docetaxel

	DOC (n=8)	Control (n=8)
Intima area, mm^2	0.15±0.13*	0.70±0.13
Media area, mm^2	0.62±0.17*	1.13±0.38
Intima-to-media ratio, %	22±18*	61±12

Values are mean±S.D. * P<0.01 vs. Control (by unpaired t-test). DOC: Docetaxel (2 mg).

4. Discussion

The major finding of this in vivo study is that, even a single low dose local delivery of DOC effectively suppresses neointimal hyperplasia.

Balloon arterial injury activates vascular smooth muscle cell migration and proliferation, thereby inducing neointimal hyperplasia [2]. This response is associated with the induction of a cascade of signaling pathways [3]. Microtubules are important in the transmission of proliferative transmembrane signals from the cell surface receptors to the nucleus [18–20]. Because of their critical role in cell signaling at multiple sites [4], microtubules can be a potential therapeutic target for antiproliferative strategies.

Taxoids, such as paclitaxel and DOC, polymerize tubulin and enhances the assembly of microtubules, and inhibit the proliferation of vascular cells [8,9], as well as tumor cells [10,11]. This inhibitory effect was reported to be sustained for a period of 14 days even after brief (20 min) application in a monoculture of vascular smooth muscle cells [9]. This may be related to its strongly lipophilic structure (facilitating rapid cellular uptake and onset of action) and its strong binding activity to tubulin (leading to sustained action) [21–23]. The recent ex vivo study demonstrated that paclitaxel substantially permeated into the vascular wall (especially into the media) even after 15 min application and that the concentration in vascular tissue exceeded the applied concentration [23]. In addition, paclitaxel affects the proliferation of endothelial cells less than that of smooth muscle cells, as shown in a co-culture experimental model [9,24].

Based on these in vitro and ex vivo findings, we examined the efficacy of in vivo application in suppressing neointimal proliferation that occurs in response to arterial injury. Taxoids were found to exert not only antiproliferative effects but also adverse hematopoietic effects (leukocytopenia) in a dose-dependent manner. The latter is the principal toxicity of this drug in vivo and therefore is of great clinical importance. To minimize the systemic adverse effects, local administration of the drug directly to the target site has been attracting increasing interest [12]. Since the local delivery of ≈35 mg of paclitaxel (using the microporous balloon over ≈30 s) did *not* inhibit intimal growth in a previous study in rabbits [9,13], we focused on DOC, an analog of paclitaxel, in the present study. This novel agent may be particularly advantageous at a low dose, because it is relatively more active as a promoter of tubulin polymerization and as an inhibitor of cell proliferation than paclitaxel [10,11].

We found that the local delivery of DOC to the injured arterial site significantly suppressed intimal hyperplasia, as shown in Table 1 and Fig. 3. This was achieved even after a single low dose (2 mg) administration. The levels of DOC in the plasma were within the ng/ml range, thus being associated with a minimal risk of leukocytopenia (Fig. 1). In immunohistochemical studies (Fig. 2), a significant decrease in smooth muscle cell proliferation but no change in endothelial cell number was observed in DOC-treated vessels. These findings indicate that the local administration of a low dose of DOC enables tissue concentrations sufficient for the cytostasis of vascular smooth muscle cells to be obtained while minimizing the likelihood of systemic side effects in an in vivo experimental model.

However, as shown in Table 1, DOC also induced a significant decrease in the medial area. This was accompanied by the reduction in cell density in the media, and documented in the previous studies using paclitaxel-coating stent [25]. These findings may indicate local toxicity, probably due to extensive injury in the vessels administered with DOC. Tissue toxicity was not observed in our previous study employing local delivery of human recombinant hepatocyte growth factor, a potent endothelial-cell mitogen, using the same experimental model [14]. Different from the re-endothelialization action of hepatocyte growth factor [13,26], the antiproliferative action of DOC may additionally disrupt normal vascular function. Moreover, this study was performed in the otherwise non-atherosclerotic arteries. In the atherosclerotic lesions, the present approach of local drug delivery may have a limitation. Therefore, further development of methods would be desirable for clinical use.

In conclusion, considering their important biological role in cell proliferation [4,5], microtubules are a therapeutic target for the prevention of restenosis following PTCA. For better efficacy and fewer adverse effects, local delivery of microtubule polymerizing agents, such as DOC, could be a potential approach.

Acknowledgements

This study was done with support from the Uehara Memorial Foundation, Osaka Heart Club and Japan Cardiovascular Research Foundation (Dr. Yasuda).

References

[1] Popma JJ, Califf RM, Topol EJ. Clinical trials of restenosis after coronary angioplasty. Circulation 1991;84:1426–1436.

[2] Bauters C, Isner JM. The biology of restenosis. Prog Cardiovasc Dis 1997;40:107–116.
[3] Foegh ML, Virmani R. Molecular biology of intimal proliferation. Curr Opin Cardiol 1993;8:938–950.
[4] Gundersen GG, Cook TA. Microtubule and signal transduction. Curr Opin Cell Biol 1999;11:81–94.
[5] Jordan MA, Wilson L. Microtubules and actin filaments: dynamic targets for cancer chemotherapy. Curr Opin Cell Biol 1998;10:123–130.
[6] Schiff PB, Fant J, Horwitz SB. Promotion of microtubule assembly in vitro by taxel. Nature (Lond) 1979;277:665–667.
[7] Gelmon K. The taxoids: paclitaxel and docetaxel. Lancet 1994;344:1267–1272.
[8] Sollott S J, Cheng L, Pauly RR, Jenkins GM, Monticone RE, Kuzuya M, Froehlich JP, Crow MT, Lakatta EG, Rowinsky EK, Kinsella JL. Taxel inhibits neointimal smooth muscle cell accumulation after angioplasty in the rat. J Clin Invest 1995;95:1869–1876.
[9] Axel DI, Kunert W, Goggelmann C, Oberhoff M, Herdeg C, Kuttner A, Wild DH, Brehm BR, Riessen R, Koveker G, Karsch KR. Paclitaxel inhibits arterial smooth muscle cell proliferation and migration in vitro and in vivo using local drug delivery. Circulation 1997;96:636–645.
[10] Riou JF, Naudin A, Lavelle F. Effects of Taxotere on murine and human tumor cell lines. Biochem Biophys Res Commun 1992;187:164–170.
[11] Garcia P, Braguer D, Carles G, Khyari SE, Barra Y, de Ines C, Barasoain I, Briand C. Comparative effects of taxol and Taxotere on two different human carcinoma cell lines. Cancer Chemother Pharmacol 1994;34:335–343.
[12] Lincoff AM, Topol EJ, Ellis SG. Local drug delivery for the prevention of restenosis. Fact, fancy, and future. Circulation 1994;90:2070–2084.
[13] Heller PF. Paclitaxel and arterial smooth muscle cell proliferation. Circulation 1998;97:1651, (letter).
[14] Yasuda S, Noguchi T, Gohda M, Arai T, Tsutsui N, Nonogi H, Matsuda T. Single low dose administration of human recombinant hepatocyte growth factor (hrHGF) attenuates neointimal hyperplasia in a balloon-injured rabbit iliac artery model. Circulation 2000;101:2546–2549.
[15] Noguchi T, Yasuda S, Itoh T, Arai T, Kanda K, Tsutsui N, Nonogi H, Matsuda T. A new multifunctional percutaneous transluminal coronary angioplasty catheter device capable of balloon inflation, local drug delivery and coronary perfusion. J Cardiol 2000;35:41–45.
[16] Vergniol JC, Bruno R, Montay G, Frydman A. Determination of Taxotere in human plasma by semi-automated high-performance liquid chromatographic method. J Chromatogr 1992;582:273–278.
[17] Aoyagi M, Yamamoto M, Wakimoto H, Azuma H, Hirakawa K, Yamamoto K. Immunohistochemical detection of Ki-67 in replicative smooth muscle cells of rabbit carotid arteries after balloon denudation. Stroke 1995;26:2328–2331.
[18] Nagata KI, Puls A, Futter C, Aspenstrom P, Schaefer E, Nakata T, Hirokawa N, Hall A. The MAP kinase kinase kinasea MLK2 co-localizes with activated JNK along microtubules and associates with kinesin superfamily motor KIF3. EMBO J 1998;17:149–158.
[19] Rosette C, Karin M. Cytoskeletal control of gene expression: depolymerization of microtubules activates NF-kappa B. J Cell Biol 1995;128:1111–1119.
[20] Alexandrova N, Niklinski J, Bliskovsky V, Otterson GA, Blake M, Kaye FJ, Zajac-Kaye M. The N-terminal domain of c-Myc associates with alpha-tubulin and microtubules in vivo and in vitro. Mol Cell Biol 1995;15:5188–5195.
[21] Straubinger RM, Sharma A, Murray M, Mayhew E. Novel Taxel formulations: Taxel-containing liposomes. Monogr Natl Cancer Inst 1993;15:69–79.
[22] Jordan MA, Toso RJ, Thrower D, Wilson L. Mechanism of mitotic block and inhibition of cell proliferation by Taxel at low concentrations. Proc Natl Acad Sci USA 1993;90:9552–9556.
[23] Creel CJ, Lovich MA, Edelman ER. Arterial paclitaxel distribution and deposition. Circ Res 2000;86:879–884.
[24] Haehnel I, Pfeifer U, Resch A, Hermann R, Schomig A, Alt E. Differential effect of a local paxlitaxel release from a biodegradable stent coating on vascular smooth muscle cells and endothelial cells in a co-culture model. J Am Coll Cardiol 1999;33:222A, (abstract).
[25] Heldman AW, Cheng L, Jenkins GM, Heller PF, Kim DW, Ware Jr. M, Nater C, Hruban RH, Rezai B, Abella BS, Bunge KE, Kinsella JL, Sollott SJ, Lakatta EG, Brinker JA, Hunter WL, Froehlich JP. Paclitaxel stent coating inhibits neointimal hyperplasia at 4 weeks in a porcine model of coronary restenosis. Circulation 2001;103:2289–2295.
[26] Morishita R, Aoki M, Nakamura S, Matsushita H, Tomita N, Hayashi S, Moriguchi A, Matsumoto K, Nakamura T, Higaki J, Ogihara T. Potential role of a novel vascular modulator, hepatocyte growth factor (HGF), in cardiovascular disease: characterization and regulation of local HGF system. J Atheroscler Thromb 1997;4:12–19.

ELSEVIER

Biomaterials 23 (2002) 3169–3174

Biomaterials

www.elsevier.com/locate/biomaterials

A novel photocurable insulator material for autonomic nerve activity recording

Toru Kawada[a,*], Yasuhide Nakayama[b], Can Zheng[a], Shoji Ohya[b], Kannna Okuda[b], Kenji Sunagawa[a]

[a] *National Cardiovascular Center Research Institute, Department of Cardiovascular Dynamics, 5-7-1 Fujishirodai, Suita, Osaka 565-8565, Japan*
[b] *National Cardiovascular Center Research Institute, Department of Bioengineering, 5-7-1 Fujishirodai, Suita, Osaka 565-8565, Japan*

Received 11 October 2001; accepted 8 February 2002

Abstract

The two-component, addition-curing silicone glue is widely used as an insulator for autonomic nerve activity recording. Due to its high fluidity before curing, a sizable mass of the glue is needed to completely cover the electrode tips, which may cause mechanical stress on the nerve. To overcome this problem, we designed a novel photocurable insulator material composed of Vaseline and 1,12-dodecanediol diacrylate (50:50 wt%) together with a photoinitiator, camphorquinone, at 0.25 wt%. This material had an appropriate viscosity of 0.18 Pa s at 25°C and was converted to a soft solid upon an arbitrary timing of photoirradiation. The compressive force per mm deformation of the resulting solid was 155.5 kPa at 1 min of photoirradiation. The impedance of the solid for 1 mm length and 10 mm^2 cross-sectional area was above 1 MΩ. In anesthetized rabbits, a very small mass of the photocurable material was able to cover the electrode tips and the nerve in situ. Changes in both the aortic depressor nerve activity and renal sympathetic nerve activity were stably recorded. These results indicate that the photocurable material developed is useful as an in vivo insulator material for autonomic nerve activity recording.

Keywords: Photopolymerization; Crosslinking; Rabbits; Aortic depressor nerve; Renal sympathetic nerve

1. Introduction

The recording of autonomic nerve activity together with cardiovascular parameters such as blood pressure and heart rate is essential to gain an insight into cardiovascular regulation under pathophysiological conditions. Bipolar metallic electrodes are frequently used for multifiber recording of autonomic nerve activity. The electrodes are attached to a surgically exposed nerve bundle and then insulated from surrounding tissues to record nerve activity. Liquid insulators such as mineral oil and liquid paraffin are used with metallic electrodes rigid enough to hold a nerve bundle [1]. However, postural changes associated with surgical preparation easily detach the electrodes from the nerve, making this method unsuitable for simultaneous recordings of autonomic nerve activities from multiple regions. On the other hand, solid insulators such as the two-component, addition-curing silicone glue are used with flexible metallic wire electrodes. Since the cured silicone glue fixes the electrode tips to the nerve and the lead wires are flexible, postural changes do not hamper the nerve activity recording. Hence, this method is useful for examining regional differences of autonomic nerve activity [2].

Despite the advantages of the addition-curing silicone glue over liquid insulators in recording autonomic nerve activity, several problems remain to be resolved. First, a pool of the silicone glue is required for the electrode tips and nerve to soak in. However, forming a proper cavity around the recording site is sometimes difficult depending on the tissue structure surrounding a given nerve. Second, the timing of curing is uncontrollable once the two components of the silicone glue are mixed. Thus, the electrode position cannot be corrected even when application of the silicone glue happens to dislocate the electrode tips from the nerve. Third, due to the high fluidity before curing, a large mass of the silicone glue tends to be formed compared to the electrode tips. Because the cured silicone glue does not adhere to the

*Corresponding author. Tel.: +81-6-6833-5012; fax: +81-6-6835-5403.
E-mail address: torukawa@res.ncvc.go.jp (T. Kawada).

0142-9612/02/$ - see front matter
PII: S0142-9612(02)00063-7